

# Investigation of concrete exposed to North Sea water submersion for 16 years

Rob B. Polder, Joe A. Larbi

TNO Building and Construction Research, Rijswijk, The Netherlands

In 1976 concrete specimens were submerged in the North Sea. Ordinary portland cement (OPC) with two water-to-cement ratios and blast furnace slag cement (BFSC) were used. After 2, 8 and 16 years specimens were investigated.

The mechanical properties of the concrete appeared not to have changed importantly due to the exposure. The microstructure and the density of microcracks were found to be normal. Sulphate, magnesium and carbonation had penetrated only the outermost few millimetres. Chloride had penetrated strongly in 16 years, depending on the cement type. Diffusion coefficients, calculated from the chloride profiles, were ten times lower for BFSC concrete than for OPC concrete. Consequently, in OPC concrete depassivation of rebars may occur within a few decades; in BFSC concrete loss of passivation can be prevented for 100 or more years.

In the specimens, reinforcement corrosion was practically absent due to lack of oxygen. Corrosion in submerged concrete can only occur in hollow air-filled structures (macrocell corrosion). In such situations the corrosion rate is probably determined by the electrical resistivity of the concrete. The resistivity was found to be much higher for BFSC concrete than for OPC concrete. This would reduce the corrosion rate in BFSC concrete macrocells significantly compared to OPC concrete.

*Keywords:* concrete, marine environment, mechanical properties, microstructure, chloride, sulphate, magnesium, diffusion, reinforcement corrosion, resistivity, cracks

## 1 Introduction

### 1.1 History

In the 1970's, the exploration of oil and natural gas in the North Sea opened a potential market for concrete off-shore structures. However, at that moment very little information was available regarding the long-term behaviour of concrete in sea water at depths exceeding a few meters. Realising this, the Dutch Foundation for Materials Research in the Sea (SMOZ), initiated a long-term exposure programme of concrete to deep sea water. Consequently, 252 concrete specimens were prepared in the TNO laboratory and exposed in the North Sea in 1976. They included variation of: concrete composition, specimen size, cover to the reinforcement, age at the start of the exposure to sea water, exposure depth. Previously, specimens were recovered after 2 and 8 years. In June 1992, the remaining 42 specimens were recovered for the final stage of the investigation, after 16 years exposure. All specimens had been exposed to a sea depth of 100 m for the first 8 years and of 40 m for the remaining 8 years. After removal of biological growth from the specimen surfaces, they were wrapped in plastic bags and stored until the start of the experiments in January 1993.

## 1.2 *Aim of the investigation*

Originally, the reason for the investigation was concern about the durability of reinforced concrete in deep sea water. The expected damage processes were reinforcement corrosion due to chloride penetration and attack of the cement matrix by sulphate or magnesium. Nowadays it is widely accepted that corrosion of reinforcement is not important in submerged concrete structures, due to negligible supply of oxygen to the steel (Arup 1983, Wilkins 1983). The only exception might be cases where aerated parts of a structure would be close to concrete exposed to sea water (like in hollow legs of offshore platforms). Furthermore, because of the positive field experience with marine concrete structures, the durability of reasonably high quality concrete in deep sea exposure is no longer questioned. Consequently the aim of the investigation was modified into describing the long-term properties, the chemical changes and the microstructure of the specimens. It was realised that the available material is unique, representing a very long exposure period, combined with a controlled and varied composition. Finally, the concrete compositions still resemble modern compositions and cements.

The objectives of the present investigation were:

- to determine the mechanical properties of the concrete;
- to determine the penetration and subsequent attack of the concrete by sulphate and magnesium;
- to analyse the chloride penetration;
- to establish the extent of corrosion of the reinforcement;
- to study the microstructure of the material;
- to determine whether the bending cracks were still present.

A literature survey of long-term deep sea and/or high pressure exposure of concrete was included to provide background information.

A full report giving more details will be published (Polder & Larbi 1995).

## 2 **Sample material**

The concrete was made in 1976 with the following compositions:

- Ordinary Portland Cement (OPC), water-cement ratio ( $w/c$ ) 0.40, 420 kg cement per  $m^3$  (composition code I);
- Blast Furnace Slag Cement with  $\approx 70\%$  slag by mass of total cementitious material (BFSC),  $w/c$  0.415, 420  $kg/m^3$  (code II);
- Ordinary Portland Cement (OPC),  $w/c$  0.54, 300  $kg/m^3$  (code III).

The age at first contact with sea water and the storage conditions until then were varied as follows:

- one week in a climate room of 20°C and 65% RH (curing code -1),
- four weeks in 20°C 65% (code -4)
- fourteen weeks, comprising of 1 week in a fog room and 13 weeks in 20°C 65% RH (code -14).

Three specimen types were made:

- plain (unreinforced) prisms  $300 \times 100 \times 100 \text{ mm}^3$ ,

- reinforced prisms  $500 \times 100 \times 100 \text{ mm}^3$ , each with 3 smooth rebars of 8 mm in diameter, which had been cleaned and etched in inhibited sulphuric acid, at 15, 30 and 46 mm cover depth,
- reinforced prisms  $600 \times 150 \times 150 \text{ mm}^3$ , with 3 similar rebars, at 20, 40 and 71 mm cover depth (this size for composition I and II only).

All reinforced specimens were bent before the exposure, until at least one crack was visible on the surface, having a width between 0.2 and 0.6 mm.

Each specimen was given a code to denote the concrete composition (I, II or III), the length of the pre-exposure storage in weeks (1, 4 or 14) and the type and size of the specimen: a and b for plain specimens, c and d for reinforced specimens of 500 mm length and e for reinforced specimens of 600 mm length.

Due to bad weather conditions at sea, the exposure of the –1 specimens could not start at the designated date and a new set had to be cast at a later date. The cements for this second set had slightly lower standard strengths. The standard strengths for the –1 specimens were  $35.4 \text{ N/mm}^2$  for the OPC and  $42.7 \text{ N/mm}^2$  for the BFSC; the standard strengths for the –4 and –14 specimens were  $44.1 \text{ N/mm}^2$  for the OPC and  $45.8 \text{ N/mm}^2$  for the BFSC.

### 3 Experimental methods

#### 3.1 General

The experiments included:

- mechanical tests: compressive strength, splitting tensile strength, dynamic modulus of elasticity,
- chemical analyses: sulphate, magnesium, sodium, potassium and chloride contents as a function of depth,
- microstructure, using polarising and fluorescent microscopy (PFM),
- corrosion: visual inspection of pits and corrosion products on the steel,
- electrical resistivity of concrete,
- crack examination using fluorescent macroscopy (FMA).

#### 3.2 Tests on plain specimens

First the electrical resistivity and the dynamic modulus of elasticity were determined. The resistivity was measured on several locations on the four faces of the prisms using a 4-electrode probe according to Wenner (Millard 1990) with 30 mm electrode spacing, placed on the concrete surface after wetting with tiny drops of a conductive gel. The frequency was 108 Hz. The dynamic modulus of elasticity was calculated from the resonance frequency determined by acoustic excitation causing longitudinal standing waves in the specimens (CUR 1960).

The samples for the mechanical and chemical experiments were cut from the plain prisms by diamond sawing, using as little water as possible. Three parts of approximately 100 mm length were sawn for compressive strength, splitting tensile strength and chemical profile plus PFM analysis respectively, as shown in Figure 1. Compressive and splitting tensile strength were determined on  $100 \times 100 \times 100 \text{ mm}^3$  cubes according to the specific Dutch standards, which includes water saturation.

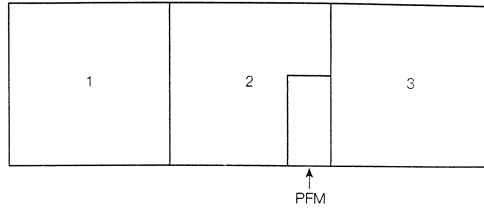


Fig. 1. Layout of samples sawn from  $300 \times 100 \times 100 \text{ mm}^3$  prisms;  
 1 sample for compressive strength testing  
 2 sample for PFM and chemical analysis  
 3 sample for splitting tensile strength testing.

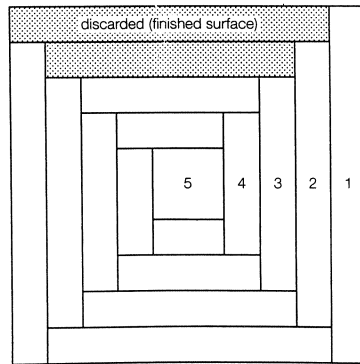


Fig. 2. Layout of slices for chemical analyses; slices next to finishing surface have not been used for the analysis (cross section).

For the chemical profile analysis, the middle parts of the prisms were sawn into slices with a total thickness of 10 mm (effectively 7 mm), parallel to the long axis of the prism as shown in Figure 2. The slices facing the finishing surfaces were discarded. Slices of similar depth were taken together as one sample and treated further after crushing and milling.

For chloride analysis a powdered sample was dissolved in hot nitric acid and titrated for chloride according to Volhard. For Na, K, and Mg, powder samples were dissolved in hot hydrochloric acid and analysed by Atomic Absorption Spectrometry. Total sulphur was tested for using a pyrolytic sulphur/carbon analyser. The aggregate/binder ratio was calculated from the total weight and the acid-soluble part, and the chemical analyses were expressed as percent by mass of cement.

From nine plain specimens a sample was taken for thin-section analysis by means of polarizing and fluorescent microscopy (PFM) as shown in Figure 1. From these, blocks of about  $50 \times 30 \times 15 \text{ mm}^3$  were sawn. After drying, they were vacuum-impregnated with an epoxy resin containing a fluorescent dye. Subsequently they were glued to an object glass, cut and ground to a thickness of approximately  $30 \mu\text{m}$ , which allows examination using polarised and fluorescent light. Polarised light allows determination of minerals; fluorescent light is especially useful for the study of porosity and microcracking.



Scanning Electron Microscopy (SEM/EDAX) analysis was carried out on three thin-sections, which were also used for PFM (the -1 specimens for each composition). Before analysis the specimens were coated with carbon, mounted onto stubs and examined using a Philips 500 SEM. This SEM was equipped with an energy dispersive X-ray analyzer (EDAX). Two samples from the surface and from the bulk of specimen II-4-a were oven-dried at about 105°C, pulverised and analysed with a Philips X-ray PW1130 diffractometer using CuK $\alpha$  radiation generated at 40 kV, 20 mA.

### 3.3 Reinforced specimens

All reinforced specimens were examined visually for cracks and other surface features. The extent of corrosion of the bars from one 500 mm specimen was visually examined after crushing the prism by compressive loading. Three 500 mm prisms showed rust spots on the concrete surface, in all cases at one end of the prism. Here the cover was broken away and the corrosion state of the rebars was examined.

Samples of the six 600 mm reinforced prisms were taken for crack examination (pattern and occurrence) and for chloride analysis. For studying the cracks a new technique was applied, called fluorescent macroscopic analysis (FMA). The samples consisted of approximately 100 × 100 × 15 mm<sup>3</sup> blocks, of which the 100 × 100 surfaces were ground and polished. After drying at about 40°C, they were vacuum-impregnated with an epoxy resin containing a fluorescent dye. The impregnated surfaces were once more polished and then examined using UV-light, which clearly shows cracks and macro-voids.

## 4 Results

### 4.1 Mechanical properties

The results of the mechanical tests of specimens after 16 years exposure are presented in Table 1. For reasons of simplicity, the numerical data of tests after 2 and 8 years are omitted. Their development as a function of the exposure duration is shown graphically in Figures 3, 4 and 5.

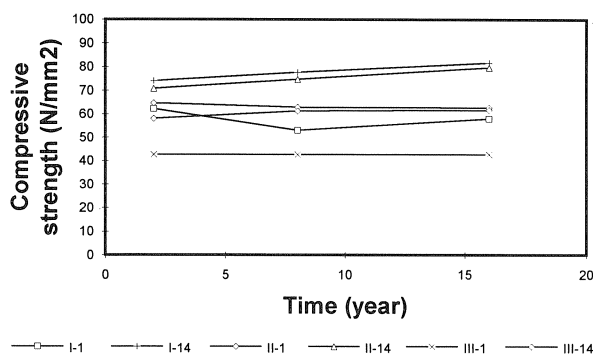


Fig. 3. Compressive strength of concrete specimens versus the length of the exposure to North Sea submersion.

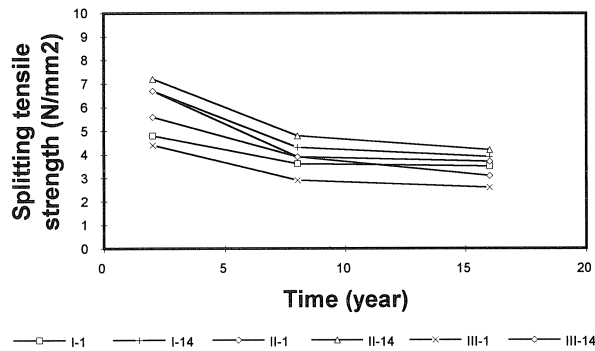


Fig. 4. Splitting tensile strength of concrete specimens versus the length of the exposure to North Sea submersion.

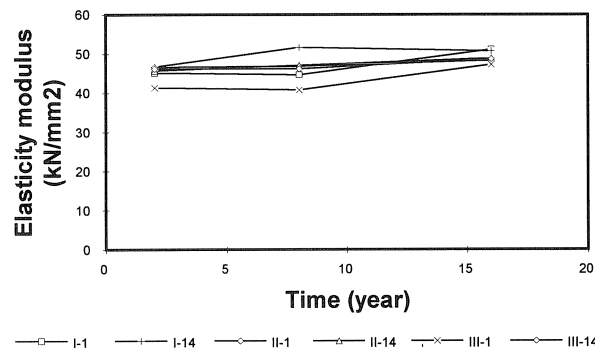


Fig. 5. Dynamic modulus of elasticity of concrete specimens versus the length of the exposure to North Sea submersion.

Table 1. Mechanical properties after 16 years.

Code	Cement type & water-to-cement ratio	Compressive strength [N/mm <sup>2</sup> ]	Splitting tensile strength [N/mm <sup>2</sup> ]	Density [kg/m <sup>3</sup> ]	E-modulus [kN/mm <sup>2</sup> ]
I-1	OPC 0.4	58.0	3.5	2420	51.1
I-4		70.5	3.0	2425	51.7
I-14		81.7	3.9	2425	50.7
II-1	BFSC 0.4	62.6	3.7	2420	48.3
II-4		81.4	4.3	2405	48.8
II-14		79.7	4.2	2410	48.8
III-1	OPC 0.54	42.6	2.6	2410	47.3
III-4		52.5	2.7	2410	47.8
III-14		61.7	3.1	2400	48.6

#### 4.2 Chemical analysis

One plain specimen of each composition, all exposed to sea water at an age of 1 week, was analysed for sulphur, magnesium, sodium and potassium. The results are shown in Table 2 and some are represented graphically in Figures 6 and 7. Due to the analysis technique used, the sulphate values may contain a contribution of sulphide as well, which may be present in significant amounts in the Blast Furnace Slag Cement concrete.

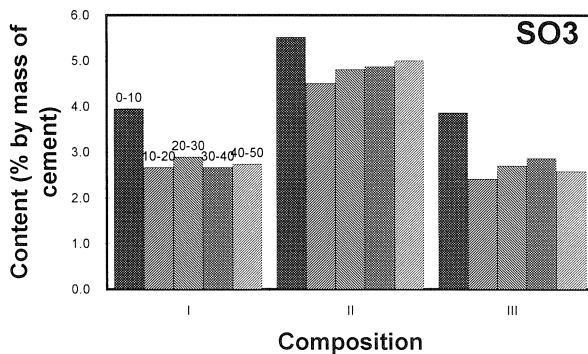


Fig. 6. Sulphate profiles.

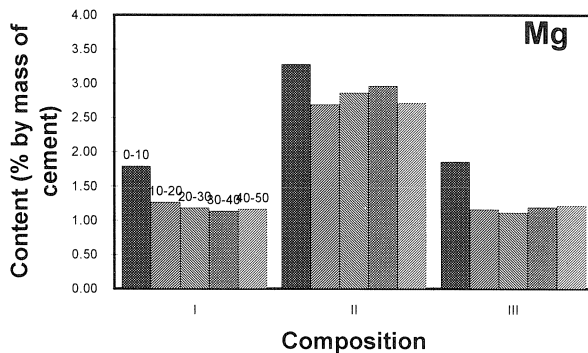


Fig. 7. Magnesium profiles.

Chloride was analysed for in nine plain prisms and in six reinforced prisms of 600 mm length. The chloride analyses generally showed strong chloride penetration, extending into the deepest part of the specimens. A diffusion profile was calculated to fit to the observed chloride profiles, resulting in an effective diffusion coefficient ( $D_{Cl}$ ) for each specimen. It was found that the best results were obtained if the chloride content of the first slice was not taken into account. Plots of chloride content as a function of depth and fitted diffusion profiles are shown in Figures 8, 9 and 10. The calculated effective chloride diffusion coefficients for each specimen, for each set with identical composition/ curing and for the average of all specimens with each composition are given in Table 3.

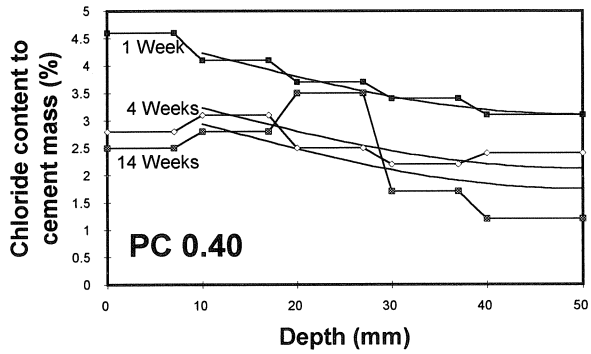


Fig. 8. Experimental chloride profiles after 16 years exposure and best fitted diffusion profiles for composition I.

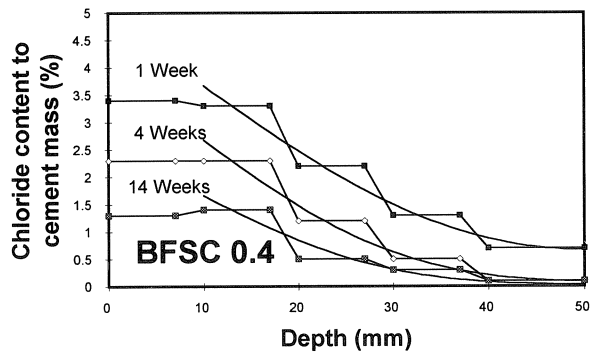


Fig. 9. Experimental chloride profiles and best fitted diffusion profiles for composition II.

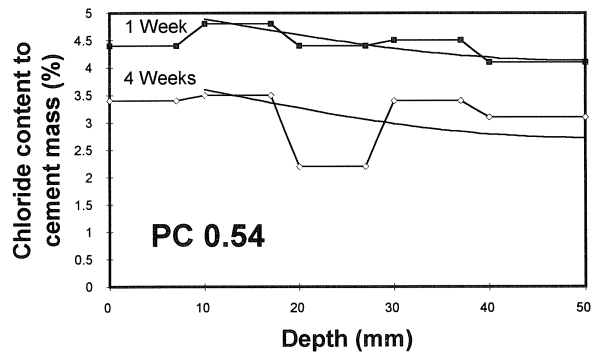


Fig. 10. Experimental chloride profiles and best fitted diffusion profiles for composition III.

Table 2. Sulphate, magnesium, sodium and potassium profiles of concrete after 16 years North Sea exposure; average (and standard deviations) of the four inner slices of the specimens; all in % by mass of cement.

Depth [mm]	1–7	10–17	20–27	30–37	40–50	10–50 average (standard deviation)
<b>SO<sub>3</sub> [% kg/kg]</b>						
I-1-a	4.0	2.7	2.9	2.7	2.7	2.7 (0.16)
II-1-a	5.5	4.5	4.8	4.9	5.0	4.8 (0.22)
III-1-a	3.9	2.4	2.7	2.9	2.6	2.7 (0.16)
<b>MgO [% kg/kg]</b>						
I-1-a	2.97	2.10	1.96	1.88	1.93	1.96 (0.08)
II-1-a	5.44	4.46	4.74	4.91	4.49	4.66 (0.21)
III-1-a	3.08	1.92	1.84	1.97	2.01	1.96 (0.08)
<b>Na [% kg/kg]</b>						
I-1-a	0.39	0.38	0.39	0.40	0.41	0.39 (0.01)
II-1-a	0.62	0.63	0.71	0.72	0.71	0.68 (0.05)
III-1-a	0.48	0.49	0.48	0.44	0.45	0.47 (0.02)
<b>K [% kg/kg]</b>						
I-1-a	0.23	0.28	0.28	0.32	0.34	0.29 (0.04)
II-1-a	0.36	0.48	0.70	0.69	0.76	0.60 (0.17)
III-1-a	0.18	0.20	0.22	0.20	0.23	0.21 (0.02)

Especially for specimens of composition III in a few cases even the “best” fitted profile appears to differ quite strongly from the measured profile. This is caused by the quite flat diffusion profiles due to the high permeability of this concrete; the degree of saturation with chloride is high. In such cases it is difficult to determine a diffusion coefficient with high accuracy. There were some individual peculiarities in the analyses as well. For III-1-a a fit based on chloride content to concrete mass, including the first layer, gave a result of  $4.0 \cdot 10^{-12} \text{ m}^2/\text{s}$ . For III-4-a the fit to chloride to concrete mass gave  $2.1 \cdot 10^{-12}$ . For III-14-a the result calculated from the chloride by mass of concrete data (without including the first layer), was  $2.4 \cdot 10^{-12}$ . All of these non-standard calculated results are marked in Table 3 with \*.

After 2 and 8 years of exposure only a few diffusion coefficients for composition II were calculated. From the profile after 2 years a  $D_{\text{Cl}}$  value of  $2.9 \cdot 10^{-12}$  was found; after 8 years exposure, 0.7 to  $1.1 \cdot 10^{-12} \text{ m}^2/\text{s}$  were found. Profiles of three specimens of composition III (first exposed at 14 weeks) determined after 8 years exposure, were calculated using the present method and gave an average value of  $3.3 \cdot 10^{-12} \text{ m}^2/\text{s}$ .

Table 3. Effective chloride diffusion coefficients  $D_{Cl}$  calculated from chloride profiles after 16 years exposure, for individual specimens, average for curing/ composition combination and average of each concrete composition.

Code	$D_{Cl}$ for individual specimen [ $10^{-12} \text{ m}^2/\text{s}$ ]	$D_{Cl}$ average for curing/ composition	$D_{Cl}$ average for composition
I-1-a	2.0	I-1:	OPC $w/c$ 0.4
I-1-e	3.5	3	I: 2
I-4-a	1.7	I-4:	
I-4-e	2.2	2	
I-14-a	1.5	I-14:	
I-14-e	0.36	1	
II-1-a	0.55	II-1:	BFSC $w/c$ 0.4
II-1-e	0.33	0.4	II: 0.3
II-4-a	0.28	II-4:	
II-4-e	0.34	0.3	
II-14-a	0.23	II-14:	
II-14-e	0.42	0.3	
III-1-a	2.7 / 4.0 *		OPC $w/c$ 0.54
III-4-a	2.8 / 2.1 *		III: 3
III-14-a	2.8 / 2.4 *		

\* see remark in text

### 4.3 Microscopic analysis

#### 4.3.1 Composition

Microscopic analysis of nine thin-sections using polarised light showed that the coarse and fine aggregates for all specimens were river sand and gravel. The gravel was composed of sub-rounded to rounded particles of quartzite and small amounts of non-porous chert and chalcedony. The sand was rich in quartz and contains a few percent of other minerals and rocks such as non-porous chert, feldspar, limestone and opaque minerals. There was no evidence of any damage to the aggregate from the sea exposure.

Specimens of series I and III were composed of portland cement; the cement of the thin-sections of series I shows a moderate to high degree of hydration; most of the  $C_2S$  grains (often existing as

clumps) have partially reacted or have not yet reacted. The cement of series III shows a somewhat higher degree of hydration. The specimens of series II are visibly composed of portland blast furnace slag cement with a moderate degree of hydration; most of the slag particles remain virtually unreacted.

The thin-section of specimens of composition I show a carbonation depth of up to about 2 mm (Photo 1). The carbonation is clearly shown as a yellowish band of concrete in which the hardened cement paste is filled with finely- divided birefringent crystals of calcium carbonate. On the surface of the specimens, small deposits of calcium carbonate,  $\text{CaCO}_3$  and sometimes brucite,  $\text{Mg}(\text{OH})_2$  and/or magnesite,  $\text{MgCO}_3$  were identified; some of these deposits were found to occur as layers on the surface and in some pores.

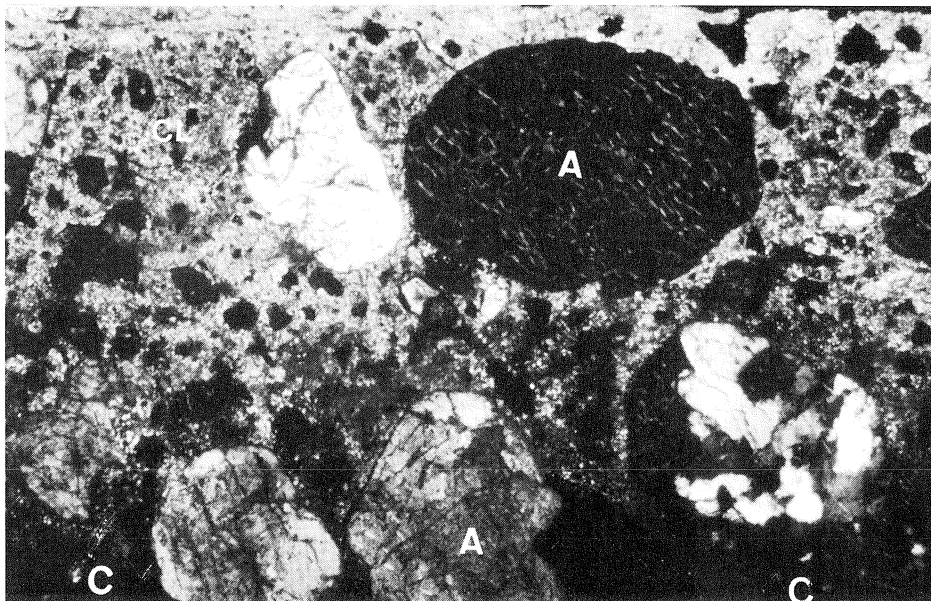


Photo 1 Overview of thin section of specimen I-1-a showing carbonation of the outermost layer (magnification 50 $\times$ ; object size 2.7  $\times$  1.8 mm<sup>2</sup>); A = aggregate; C = cement paste (not carbonated); CL = carbonated layer (light yellow in colour).

The thin-section of specimen II-1-a shows that the concrete is carbonated to a depth of about 0.5–1 mm. The deposits on the surface of this specimen are the same as those of series I but they occur in lesser amounts. The depth of carbonation of specimen II-4-a is 1.5 to 2 mm. There were hardly any deposits of calcium carbonate, brucite, magnesite identified in or at the surface. Specimen II-14-a is very similar. In general, the concrete of composition II is of good quality and chemically unchanged.

The concrete of III-1-a was carbonated to a depth of about 0.5 to 2 mm. It showed well defined layers of calcium carbonate, brucite, magnesite and in some cases gypsum (Photo 2). Magnesite and ettringite crystals also occur commonly in most of the voids and microcracks in the outer 2–7 mm. The concrete of specimen III-4-a was found to contain a relatively high amount of pores (air-voids) of a broad size-range (from  $< 10 \mu\text{m}$  up to about  $50 \mu\text{m}$  in diameter). On the surface and in some voids (a few millimeters from the surface), small amounts of calcium carbonate, ettringite, brucite and magnesite were identified either separately, occurring as layers or inter mixed with each other. Ettringite was identified mainly in voids a few millimeters below the surface of the concrete. Specimen III-14-a had a relatively open structure and contained irregularly-formed pores different from the air-voids that was observed in specimen III-4-a. No evidence of chemical changes was identified.

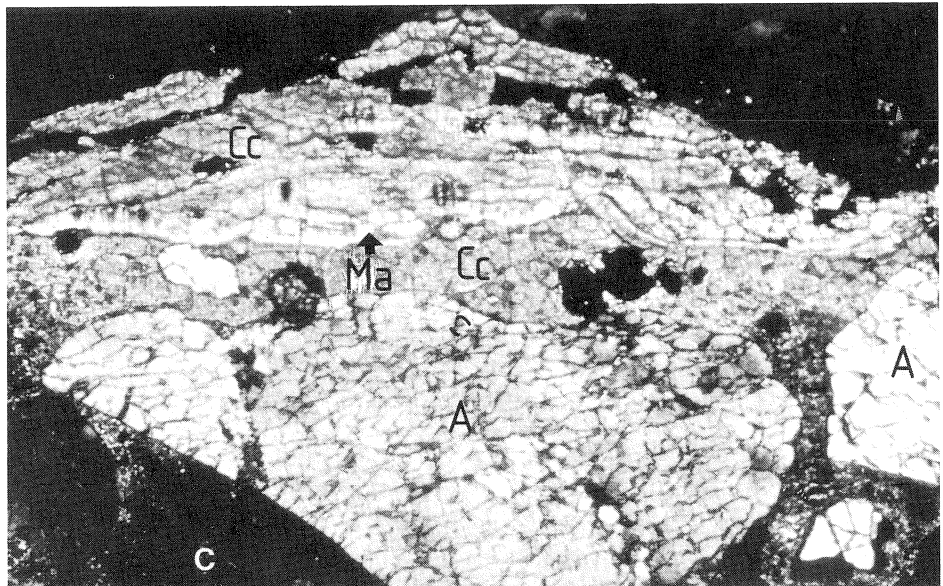


Photo 2 Thin-section micrograph showing deposits of calcium carbonate ( $\text{CaCO}_3$ ), and magnesite ( $\text{MgCO}_3$ ) directly on the surface of specimen III-1-a (magnification = 200 $\times$ ; object size  $0.7 \times 0.45 \text{ mm}^2$ ); Cc = calcium carbonate; Ma = magnesite; C = not carbonated cement paste.

#### 4.3.2 Microstructure

Fluorescent light microscopy of thin-sections showed that the cement paste for the nine specimens had a homogeneous microstructure (see for example Photo 3); specimens of the series I and II have denser cement pastes than those of series III. It was observed that the carbonated surface layers were denser than the uncarbonated cement paste (Photo 4). Also remarkably, these carbonated zones do not contain microcracks. Normally, microcracks are common in the surface layers of concretes (not exposed to deep sea) as a result of shrinkage during hardening. Their absence in the present specimens suggests that existing microcracks (prior to the sea exposure), have been blocked or filled partly by the carbonation of the concrete. Deposition of products of reaction between the concrete and the sea water, as described above, may have contributed to this process. This deposit is



likely to reduce the surface permeability of the concrete and thereby reduce the exchange of materials between the sea and the concrete.

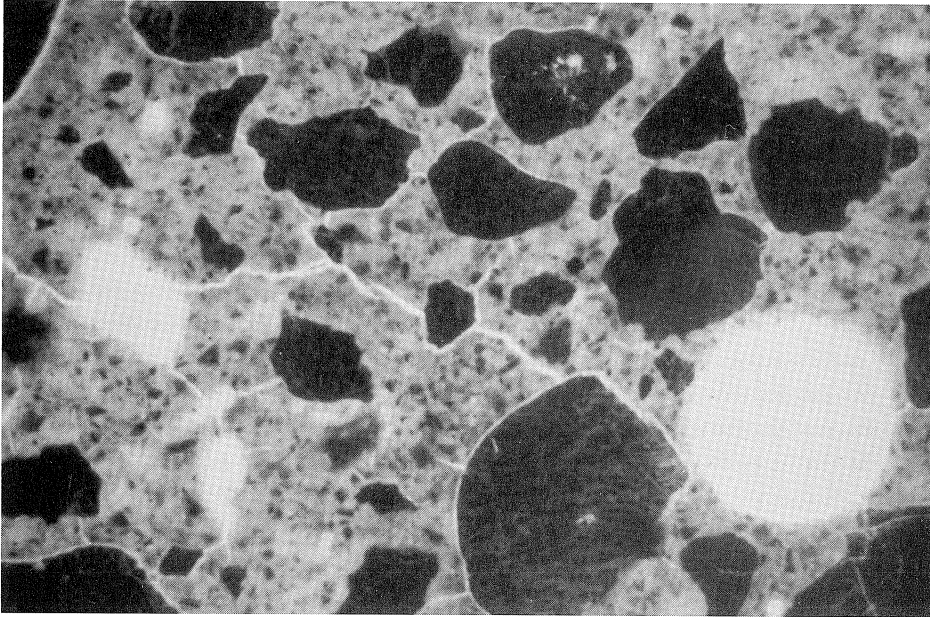


*Photo 3 Bulk of specimen II-4-a in fluorescent light showing microcracking in a homogeneous cement paste (magnification = 100×; object size 1.4 × 0.9 mm<sup>2</sup>).*

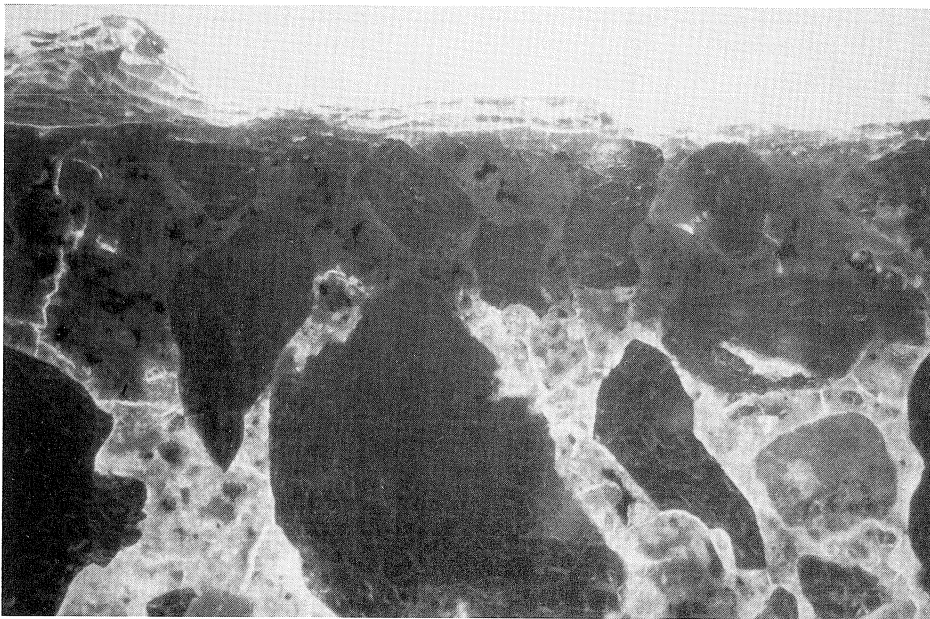


*Photo 4 Surface layer of specimen III-1-a in fluorescent light; the carbonated cement paste (CL) is denser (darker) than the not-carbonated part (magnification = 100×; object 1.4 × 0.9 mm<sup>2</sup>).*

### 4.3.3 Microcracks

The cement paste of all examined thin-sections contained microcracks with a density in the range of 15-40 microcracks/mm<sup>2</sup>. An example is given in Photo 3. These microcracks occur mostly as adhesion cracks in the interface between aggregate particles and the cement paste; their widths range between 5 and 10 μm in the cement pastes up to about 15 μm at the interface of the aggregate particles. In the three BFSC specimens, a slightly higher density of ≈ 30–40 microcracks/mm<sup>2</sup> was registered than in the OPC samples. Just as many of these microcracks occur in the cement paste as along the paste-aggregate interface.

To study this further, a similar crack density analysis was made of samples made with similar BFSC of various ages but not exposed to deep sea. One sample concerns a core from an at least 5 years old drinking water tank; two samples were taken from laboratory cubes exposed in a fog room for two months. The results have been presented in Table 4. They show a density of microcracks for the mature specimen exposed to drinking water, that is similar to those exposed to deep sea. For the younger (fog room) specimens, the crack density was found to be lower. Furthermore, it was observed that the widths of the microcracks in the younger specimens were smaller than those in the older ones. The widths range from < 5 μm (in the cement paste) to about 15 μm (at the interface of the aggregate particles). Most of these microcracks were not interconnected with each other.

Table 4. Density of microcracks in various concretes made with ordinary portland cement (OPC) and blast furnace slag cement (BFSC).

Type of specimen	Water-cement ratio ( <i>w/c</i> )	Age	Number of microcracks per mm <sup>2</sup>
This investigation I or III (OPC)	0.40; 0.54	16 years	15–40
This investigation II (BFSC)	0.40	16 years	30–40
Core from a water storage tank (BFSC)	c. 0.45	> 5 years	28
Fog room cured cube (BFSC)	0.40	2 months	16
Fog room cured cube (BFSC)	0.55	2 months	12

### 4.3.4 SEM / EDAX and XRD analysis

The SEM analysis confirmed the features that were identified from the PFM investigations, including for example magnesite deposits in pores. No crystals of sodium chloride (NaCl) were identified. The amount and distribution of chloride (Cl) were virtually the same throughout the specimens, reflecting a homogeneous distribution.

The XRD spectra of the samples from the surface and from the bulk of specimen II-4-a, were very similar. The following minerals were detected in both: Quartz, Ettringite, Portlandite,  $(\text{Ca}(\text{OH})_2)$ . Only the surface sample contained calcite (calcium carbonate). No chloride-containing phase nor brucite were identified.

#### 4.4 Concrete resistivity

From the resistance measurements made on the concrete surface, the resistivity values were calculated according to the theory of Wenner, multiplied by a correction factor of 0.8 which was found in previous laboratory research (Tondi et al. 1993). In Table 5, the average resistivity of two specimens with identical composition and curing are given as well as the overall average resistivity of each concrete composition. The average coefficient of variance for all surface resistivity measurements was 25%.

#### 4.5 Corrosion of rebars

The visual examination of the bars taken from the demolished specimen III-1-d showed only superficial and local corrosion with one pit on each of the bars; the maximum pit depth was about 0.5 mm and the maximum pit size was about  $3 \times 5 \text{ mm}^2$ . Three prisms showed rust spots on their surface. In all cases, it turned out to be minor corrosion on the end faces of the rebars, with low cover to the bars. In one case (I-1-c) the end surface of the bar had a cover of 10 mm from the end face of the prism. In prism I-14-c the bar end that showed corrosion and had apparently caused some cracking, had a cover of 14 mm from the prism end face. Prism II-1-c showed tiny rust stains on the surface. After breaking away the thin concrete layer covering the plastic studs used for fixing and spacing the rebars, rust spots were found on the stud of the 15 mm cover bar near the end face of the prism. Apart from the specimens mentioned above, none of the prisms showed any sign of corrosion on the concrete surface.

Table 5. Concrete resistivity after 16 years North Sea exposure; for each combination of composition and age at start of exposure and overall average for the three compositions.

Composition – age at start of exposure to sea water	Resistivity [ $\Omega \text{ m}$ ]	Average resistivity for concrete composition [ $\Omega \text{ m}$ ]
I-1	109	OPC 0.4
I-4	155	155
I-14	202	
II-1	426	BFSC 0.4
II-4	612	675
II-14	990	
III-1	90	OPC 0.54
III-4	118	120
III-14	160	

#### 4.6 Crack examination

The surfaces of all 24 reinforced specimens were inspected visually for cracks. Three specimens showed no cracks. Of the others, the specimens with concrete composition I and II had crack widths on the surface from less than 0.1 to 0.5 mm. Composition III specimens showed only very fine cracks of less than 0.1 mm width. Initially (in 1976), all specimens had at least one crack of 0.2 to 0.6 mm wide. As the information on the original crack widths of individual specimens was lost, the surface cracks after 16 years can only be compared in a general sense. It appears that all crack widths on the surface have decreased to roughly half their initial value.

In order to study the cracks inside the concrete, three  $600 \times 150 \times 150 \text{ mm}^3$  and one  $500 \times 100 \times 100 \text{ mm}^3$  specimens were selected for macroscopic examination of their cross section. Due to the vacuum-impregnation of the specimens with a fluorescent resin, all cracks and voids were clearly visible under UV-light. In the three specimens of 150 mm section a major crack ( $\approx 0,2\text{-}0,4 \text{ mm}$  wide) traversing the entire width of the specimen, sometimes with a number of smaller cracks branching off was observed. For specimen II-1-c (100 mm section) the crack width inside was about 0.1 mm; it was very fine ( $<0.1 \text{ mm}$ ) on the outside. The cracks appeared to run mainly through the cement paste and the paste-aggregate interfacial zone. In most cases the crack width increases where the cracks run along the aggregate particles. As an example, Photo 5 shows these features.

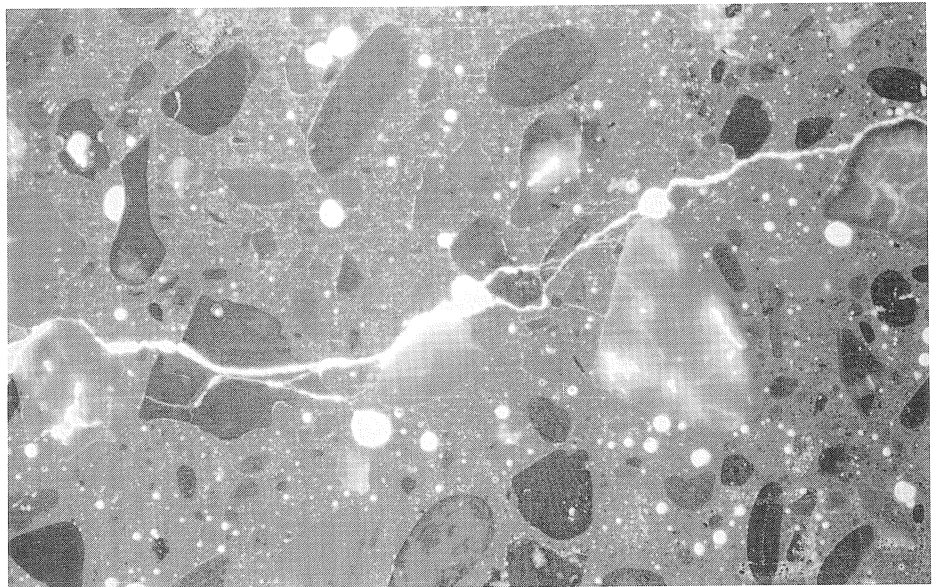


Photo 5 Cross-section of specimen II-14-e showing bending crack from the surface (left) to the centre (right); photo taken under UV-light after impregnating with fluorescent resin (Fluorescent Macroscopy Analysis); object size  $100 \times 75 \text{ mm}^2$ .

## 5 Survey of related literature

### 5.1 *US hollow sphere exposure programme*

Since 1971, the US Naval Civil Engineering Laboratory has been conducting a programme of deep sea exposure of concrete (Rail & Wendt 1985). Hollow spheres with a diameter of 1.6 m and a wall thickness of 103 mm were made with 435 kg/m<sup>3</sup> OPC and a water-cement ratio of 0.40. They were exposed at ages from 3 to 21 weeks at depths between 550 and 1550 m near the coast of California. Some of the spheres were coated and some were reinforced. Control prisms were kept in a fog room, stored in outdoor atmosphere and exposed together with the spheres. The spheres have been inspected annually by divers. After 5.3 and 10.5 years some have been retrieved and tested.

The results of the investigation can be summarised as follows:

- Concrete strength had not decreased importantly due to the deep sea exposure for 5 or 10 years, although the compressive strength was generally 15% lower than that of control specimens;
- The modulus of elasticity was essentially constant;
- The water uptake, which is a measure of the permeability for sea water, was relatively rapid during the first year but then slowed down;
- The microstructure of the concrete appeared practically unchanged; magnesium was not found in significant quantities in the material.
- No corrosion of the reinforcement was observed.

### 5.2 *High pressure sea water laboratory investigation*

A series of investigations was carried out in The Netherlands by CUR of concrete in sea water under high pressure (Bijen & Van der Wegen 1992). Concrete and mortar specimens were exposed in a pressure vessel containing artificial sea water or saturated lime solution at 100 bar. Companion specimens were exposed at 1 bar. The cement types were OPC and BFSC, which were similar to those in the present investigation.

Mechanical testing (compressive and tensile strength, dynamic modulus of elasticity) of mortar prisms showed no effects of the high pressure up to 6 months exposure duration. It was concluded that the stability of the material had not been adversely affected. Penetration of chloride and sodium and leaching out of potassium was observed, which were faster under high pressure than under atmospheric pressure; faster for OPC than for BFSC specimens; and faster for higher water-to-cement ratios (0.50 versus 0.40). The water permeability under high pressure was found to have decreased with time in sea water; this was probably due to the formation of brucite and calcite/ aragonite in the outer layers. The concrete was found to swell more and faster under high pressure than under atmospheric pressure. In saturated lime water, the swelling was found to be less than in sea water.

### 5.3 *Extreme high pressure experiments*

Concrete testing under water pressures up to 600 bar showed loss of strength, but the degree of loss depended strongly on the test method (Clayton 1986). The compressive strength of 100 mm cubes after 6 days at 600 bar fell to about 88% compared to control specimens. The flexural strength of

300 × 90 × 90 mm<sup>3</sup> prisms was found to decrease to about 50% after the same exposure. A gas pressure tensile strength test showed to be most sensitive to the effects of high pressure exposure: after the same exposure 200 mm × 100 mm cylinders showed a reduction of the “gas pressure tension strength” (GPTS) to 15% of the control values. This extreme sensitivity of the GPTS test is related to changes in the microstructure of the material, probably of the interaction between coarse aggregate and cement paste. Thin-section microscopy showed extensive micro-cracking, predominantly along the coarse aggregate-mortar interface.

From the gas pressure tension test, the following influence of several variables was found:

- Lower pressure (30 bar) resulted in much lower strength loss; the GPTS was found to be 90% of the control values.
- The strength loss was most severe for exposure times over a few hours.
- No effect was found of the rate of pressure release.
- Flexural strength testing of prisms inside the pressure vessel at 600 bar, showed that the strength loss occurred before depressurisation, apparently as a direct result of applying the high water pressure.

#### 5.4 *Five years exposure of concrete at 140 m depth*

Within the UK programme Concrete in the Oceans, concrete prisms have been exposed up to 5 years at 140 m depth (Stilwell 1988). The concrete was made with OPC, including a standard-grade mix with  $w/c = 0.45$ , 435 kg cement/m<sup>3</sup>; and a low-grade concrete with  $w/c = 0.65$  and 305 kg/m<sup>3</sup>; a third mix was made with OPC and 20% pulverised fuel ash (PFA) and a water-to-(cement + PFA) ratio of 0.44. Specimens were recovered after 2.5 and 5 years.

Compressive strength after exposure at 140 m was found to be about 80 to 90% of the control specimen strength. Thin-section microscopy showed an increase in microcracks of about 20 micrometer width after exposure, mainly around coarse aggregate particles; control specimens showed only microcracks of about 5 micron width. Considerable chloride penetration was found. In plain OPC concrete after 5 years exposure chloride contents were found from 1.5 to 2.0% by mass of cement (standard grade) up to 2.0 to 2.7% (low grade concrete). No corrosion of reinforcement and no deterioration of concrete was found. Concrete resistivity was measured after exposure; low grade concrete had a resistivity between 70 and 100 Ω m, standard grade about 120 Ω m, both after 5 years; PFA concrete had a resistivity of about 700 Ω.m after 2.5 years exposure. These resistivities were lower than laboratory (wet) stored control specimen resistivity values.

## 6 Discussion

### 6.1 *Mechanical properties*

The compressive strengths after 16 years exposure of all three concrete compositions were comparable to the values after 2 and 8 years. Apparently no important changes of the compressive strength have occurred during the exposure. It appears that a higher age at the start of the exposure to sea water is slightly favourable for a high compressive strength. For instance, the strength of

concrete of mix I exposed at 14 weeks is about 80 N/mm<sup>2</sup> and of exposed at 4 weeks it is 70 N/mm<sup>2</sup>. The strength of composition I exposed at 1 week (58) is lower because of the lower standard strength of the cement. The same trend exists in the strength of mixes II and III.

The splitting tensile strength results of specimens exposed for 16 years were in general slightly lower than those of concrete exposed for 8 years; both were lower than the results after 2 years exposure. Although taken strictly it may be incorrect to average all data of a certain age, doing so provides a general way for comparison. The average 16 year value of the splitting tensile strength was 58% of the 2 year average value, the 8 year average result was 64% of the 2 year average level. Apparently the relatively strong decrease from 2 to 8 years had not continued, but had rather stabilised. The splitting tensile strength decrease in time appears to reflect a negative effect of exposure to sea water, which was not shown by the compressive strength, similar to what has been found by (Clayton 1986). As apparent deterioration of the microstructure was absent, there is no definite explanation for the tensile strength decrease. It may be related to swelling phenomena observed in the high pressure sea water experiments (Bijen & Van der Wegen 1992).

The dynamic modulus of elasticity was in all cases found to be slightly higher after 16 years compared to values after 2 and 8 years, which were very similar. There was no effect of the age at the start of the exposure on the elasticity modulus. Apparently the modulus is not a sensitive measure of changes occurring in the concrete during sea water exposure.

## 6.2 *Chemical analysis*

### 6.2.1 Sulphate and magnesium analyses

The sulphate results of three specimens exposed at an age of one week showed an increased sulphate content in the first 7 mm only. Deeper layers all had very similar sulphate contents, which can be regarded as the bulk content, originating from the particular cement used. As the penetration of sulphate in specimens with longer pre-exposure storage (4 or 14 weeks) was expected to be less deep, they were not analysed for sulphate. Microstructural examination proved this to be right.

Generally the same applied to the magnesium as to the sulphate results. Apparently the penetration of magnesium has been limited to the outermost 7 mm of the concrete. No signs of attack were found.

### 6.2.2 Sodium and potassium analyses

Sodium has quite flat "profiles" in the OPC concretes. Hypothetically, this may result from either saturation with sodium for the sea water, or from the absence of penetration or leaching of sodium. As the III concrete, which is more porous, contains more sodium than the I mix (0.47 to 0.39%), it appears that the sodium content is determined by more or less complete equilibration with penetrated sodium. This suggests that no Na is bound to solid phases in the OPC concrete, either penetrated from the sea water or originally present. The sodium content in the BFSC concrete is higher than in the OPC concrete, probably because quite some (originally present) sodium remains bound in the slag particles.

The potassium is slightly lower in all outer layers, suggesting some leaching out. The profile in the BFSC concrete is steeper than in the OPC concretes, which agrees with a lower diffusion coefficient (just as well for potassium as for chloride) than for OPC concrete; furthermore some K probably remains bound in the slag particles.

### 6.2.3 Chloride analysis

The results of the chloride analysis showed strong chloride penetration into specimens made with OPC. The BFSC concrete showed only limited penetration. The effective diffusion coefficients found in the fitting procedure are substantially lower for BFSC (composition II) than for OPC, with slightly lower values for OPC with  $w/c$  0.40 (I) than with  $w/c$  0.54 (III). Generally there was a small influence of the age at the start of the exposure on the diffusion coefficient; a higher age seemed to reduce it somewhat. This may be explained by a higher density of the surface layer due to longer hydration before exposure to sea water and subsequent sea water uptake. The diffusion coefficients were found to agree well previous experience. In particular the development in time of the BFSC diffusion coefficients fits well with the findings of a recent literature survey on long term chloride diffusion data (Bamforth 1994).

The fact that less chloride penetration was found in association with a higher age at the start of the exposure, gives a clue to the nature of the transport mechanism. The possibilities are capillary absorption and diffusion. Higher age (while stored in 20°C and 65% RH) before exposure means deeper drying out, so stronger capillary absorption. If chloride ingress would have been dominated by capillary absorption, this would have resulted in a higher chloride content in the longer cured specimens. Although this may have been the case in the first period of exposure, it was not after 16 years and also not after 2 or 8 years. Consequently, it is clear that after say a few years, diffusion takes over as the dominating transport process. This is in agreement with data from 6 year exposure tests in marine splash zone, where diffusion was found to be dominant after about one year (Bamforth & Chapman-Andrews 1994).

A remark may be made regarding chloride binding here. If chloride from sea water would only penetrate and it would not be bound, the concrete would contain about 0.7 to 1.0% chloride by mass of cement. Now the highest chloride contents found after 16 years are much higher (2 to 5%). This can only be explained by assuming that extensive chloride binding has occurred. Binding of chloride ions from the pore solution to solid cement phases reduces the chloride ion activity in the solution, allowing new chloride penetration from the sea water by diffusion, which is driven by the activity (concentration) difference. Eventually, there will be an equilibrium between the solid chloride phases, the pore solution and the sea water. Assuming equilibrium between sea water and pore solution, which is reasonable after 16 years (at least for the outer layers), the ratio of bound to free chloride may be calculated. It is about 4 to 1 for concrete with composition I, and 3 to 1 for specimens of composition II and III. In other words, at least 75% of the total chloride is bound to solid phases.

It is remarkable that no crystalline chloride containing phases could be detected inside the concrete. Apparently the chloride is bound to the C-S-H gel, which is supported by the general presence of chloride found with EDAX. C-S-H-chloride combination products are not crystalline and consequently cannot be detected by X-ray diffraction.



Generalising the chloride penetration data, the average time-to-depassivation (ttd) for steel embedded in each of the three mixes was calculated. Inputs were the observed chloride diffusion coefficients and the assumption that 1% chloride ion by mass of cement is the critical chloride content for loss of passivation. The results for three depths of cover are indicated in Table 6. Using BFSC and a cover to the steel of 50 mm, the reinforcement may become depassivated after about 100 years. It appears impossible to obtain a ttd of more than a few decades with OPC concrete.

Table 6. Average time to steel depassivation in years for the three investigated concrete mixes and three cover depths, assuming a critical chloride content of 1% chloride ion by mass of cement.

Cement type, $w/c$	OPC, 0.4	OPC, 0.54	BFSC, 0.4
DCI [ $\text{m}^2/\text{s} \cdot 10^{-12}$ ]	2.0	3.0	0.3
cover [mm]	time-to-depassivation [year]		
30	5	4	36
50	15	10	100
70	30	20	200

### 6.3 Microstructure

As far as the microstructure concerns, chemical interaction between the sea water and the concrete has been confined to the outermost 2 mm in the “high quality” concrete compositions (I and II) and to the outer 7 mm of the “low quality” concrete of composition III. The changes relate to carbonation of the cement paste and reaction with magnesium and sulphate ions. These “penetration depths” represent the specimens which were exposed at the youngest age. The effect on the microstructure of a higher age at the start of the exposure was small for compositions I and II. For the “low quality” OPC concrete of composition III, the effect of higher age at first contact with sea water seemed to reduce the penetration.

The number of microcracks found with fluorescent microscopy showed no important differences between concrete compositions within this investigation. Microcrack densities of specimens from other sources were determined for comparison. A sample of BFSC concrete which had been exposed to pure water for about 5 years showed the same microcrack density as the specimens exposed to sea water for 16 years. Young BFSC concrete kept in a fog room, which had not been subjected to any stresses (thermal, drying shrinkage, mechanical loading), showed a lower microcrack density. It may be inferred that the microcrack density found in the specimens exposed to sea water for 16 years may be considered normal for mature concrete in wet conditions.

#### 6.4 Corrosion related properties

The amount of chloride and its depth of penetration in the specimens mean that most of the embedded steel bars have lost passivation. Depending on the exact critical chloride content, all bars in OPC concrete (compositions I and III) up to 70 mm cover depths and those with lowest covers (15 to 30 mm) in BFSC concrete (composition II) must be assumed to have depassivated. On the other hand, it is well known that the actual corrosion rates of steel in concrete that is completely submerged in sea water are very low, due to the limited access of oxygen through the concrete cover (Arup 1983, Wilkins 1983). The practical absence of corrosion in the specimens confirms this, in agreement with the experimental findings of (Stilwell 1988).

The amount of corrosion observed was negligible; the corrosion pits found on the reinforcement bars of the demolished specimen have probably been active during the early stages of the exposure, when the concrete still contained some oxygen. The corrosion stains found on the surface of a few specimens are completely related to low cover to the bars (<15 mm) and are most probably caused after retrieval of the specimens from the North Sea. During the storage before the actual start of the investigation, some oxygen may have penetrated and activated corrosion of the steel bars with the lowest cover.

Despite the absence of corrosion in the specimens, it may be useful to consider the potential risk of corrosion in cases where parts of a marine structure are aerated (close to parts with high chloride penetration). This may be the case in hollow legs of offshore structures, where so-called macro-corrosion cells could develop, with the active anodes in the chloride containing concrete and the cathodes on the aerated side of the concrete wall, as schematically shown in Figure 11. In such cases the electrical resistivity of the concrete mainly determines the effective cathodic area and consequently the corrosion rate (Raupach 1992).

There appeared to be two main influences on the resistivity values found:

- the concrete composition; the resistivity of BFSC concrete (composition II, overall average 675  $\Omega\cdot\text{m}$ ) was higher than that of OPC concrete with  $wcr$  0.4, (composition I, average 155), which was in turn higher than that of OPC concrete with  $wcr$  0.54, (III, average 120);
- the age at first exposure to sea water; the resistivity of all specimens cured for 1 week before the exposure was lower than that of specimens with the same composition cured for 4 weeks, which was also lower than the values of specimens cured for 14 weeks.

The dependence of the resistivity of water saturated concrete on the composition (cement type, water to cement ratio) is well known; it is mainly related to the pore structure. In order to examine the influence of the sea exposure on the resistivity, the results may be compared to those from previous work on concrete resistivity (Polder & Ketelaars 1991). That investigation involved OPC and BFSC concretes of water to cement ratios of 0.65, 0.55 and 0.45, a maximum grain size of 16 mm and a cement content of 325  $\text{kg}/\text{m}^3$ . Specimens were 150 mm cubes containing four pairs of brass electrodes at different depths, for resistance measurements. The cubes were cured in a fog room for four weeks and subsequently exposed to climate rooms of 20°C between 50%, and 90% R.H., in a fog room or immersed in (tap) water. From (Polder & Ketelaars 1991) data are available up to 1.9 years

of concrete age; later measurements up to 3.8 years are given here. The values given are averages of measurements on two cubes and a total of eight electrode pairs. The results are shown in Table 7.

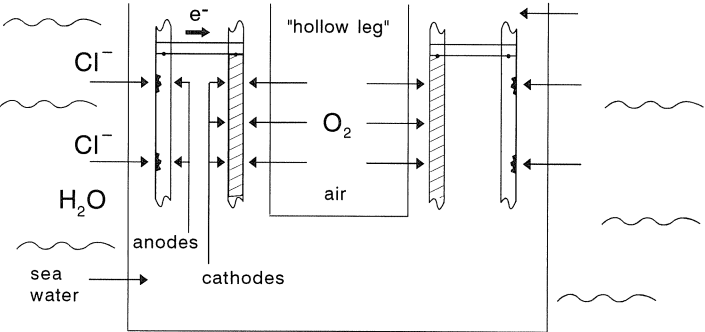


Fig. 11. Schematic representation of macrocell corrosion in a hollow, air-filled submerged structure.

Table 7. Concrete resistivities from this investigation and from laboratory experiments (Polder & Ketelaars 1991), in  $\Omega \cdot m$ .

	Age at start of exposure				Laboratory (Polder & Ketelaars 1991)		
	1 week	4 weeks	14 weeks	overall average	Age	1.9 year	3.8 year
16 years North Sea							
Composition	Resistivity [ $\Omega \cdot m$ ]				Composition	Resistivity [ $\Omega \cdot m$ ]	
I	110	155	200	155	OPC 0.45	150	180
II	425	610	990	675	BFSC 0.45	480	550
III	90	120	160	120	OPC 0.55	110	125

Generally there is good agreement between results of comparable concrete compositions. The resistivity of OPC *wcr* 0.4 concrete is somewhat low compared to the results from the laboratory after 3.8 years; the BFSC concrete values are somewhat higher and the OPC *wcr* 0.54 values are very similar to resistivities of comparable concrete in the laboratory. Possibly the laboratory resistivities will increase somewhat in the course of time due to further hydration, as is suggested by the slight increase from 1.9 to 3.8 years. In that case it may be concluded that in the long term both sea exposed OPC concrete compositions have a somewhat lower resistivity than concrete cured in pure water environment. Considering this, the OPC resistivity values may have been reduced slightly by the increased chloride content of the pore water.

The resistivity of BFSC concrete specimens after 16 years sea water exposure are well above those from the laboratory after 1.9 to 3.8 years, except that of the specimen which was exposed at an age of one week. It may be inferred that only in this case the chloride penetration into the concrete has significantly reduced the resistivity of the BFSC concrete.

The effects are small, however. Generally it may be concluded that the sea exposure has had no major influence on the electrical resistivity of the concrete.

The reason for investigating the resistivity of the specimens was its relation with corrosion of reinforcing steel (after depassivation). A simplified approach of the influence of concrete resistivity, based on the work of Bazant in the late 1970's, states that the corrosion rate is inversely proportional to the resistivity (Polder 1990). More recent experimental and theoretical work has shown that in reality the situation may be more complicated (Raupach 1992, Polder et al. 1994). It is obvious from the electrochemical nature of the corrosion process, however, that the higher the resistivity, the stronger its mitigating influence on the corrosion rate is. A relatively simple relationship may only exist in macrocell corrosion in hollow air filled structures.

In particular in macrocell situations, steel corrosion rate in BFSC concrete exposed to sea water may be expected to be substantially lower than in OPC concrete because the resistivity is about 4 to 6 times higher (for similar curing).

#### 6.5 *Cracks*

The flexural cracks produced before the exposure were still present in the specimens after 16 years exposure to sea water. Macroscopic examination suggests there was no significant decrease of the crack widths. Despite the moist exposure conditions, apparently there has not been any healing of the cracks due to cement hydration or due to formation of deposits of reaction products between sea water and pore water. Healing of cracks may take place only where water flow through the cracks occurs.

## 7 **Conclusions**

The investigation described here has confirmed the findings of studies by other researchers and adds more quantitative information to support them. The value of the present work lies in the fact that the results are obtained from concrete that has been exposed to natural sea water for 16 years. It must be realised, however, that the investigation has addressed only concrete which was completely and permanently submerged in sea water. The findings do not necessarily apply to concrete in the splash zone. The conclusions can be summarised as follows.

1. Permanent immersion in sea water is not a severe environment for plain and reinforced concrete. No rust was detected on the reinforcing bars, whether in the precracked nor in the uncracked areas, although no significant healing of the cracks was observed.
2. The compressive strengths and the dynamic elastic modulus had remained practically constant throughout the entire exposure period, at levels to be expected for the various concrete

compositions involved. The drop of splitting tensile strength observed between 2 and 8 years remained unexplained; it was not caused by deterioration of the microstructure of the concrete. This is in general agreement with literature data.

3. The microstructure of the concrete, including the microcrack density, was found to be normal. No deterioration was observed. Compositional changes due to reaction with sulphate and magnesium from the sea water were restricted to a depth of 2 to 7 mm from the concrete surface. Superficial carbonation was found, which was probably due to biological activity.
4. Chloride was the only sea water component that had penetrated the concrete deeply. The penetration depth was strongly influenced by the cement type and to a minor extent by the water-to-cement ratio and by the age at which the concrete was brought into contact with sea water. Chloride diffusion coefficients for BFSC concrete were found which were about one order of magnitude lower than for OPC concrete. This is in agreement with various other laboratory and field investigations.
5. During the exposure most of the embedded steel had lost passivation. However, in the specimens investigated, reinforcement corrosion was practically absent because of the very limited transport rate of oxygen through the water saturated concrete.
6. The electrical resistivity of specimens made with BFSC was much higher than the resistivity of OPC specimens, in general accordance with laboratory data. It was found that the exposure to sea water has not changed the electrical properties of the concrete very much. A higher concrete resistivity may be significant in reducing the corrosion rate in structures where so-called macrocell corrosion occurs. This may be the case inside air-filled hollow legs of offshore platforms, where steel in aerated concrete is at close distance to steel which has become depassivated due to chloride ingress (on the outside of these structures). If the concrete in this investigation would have been (partially) aerated, significant corrosion rates of the reinforcement would have been possible. In such cases, the higher electrical resistivity of the Blast Furnace Slag Cement concrete would probably reduce the corrosion rate significantly compared to Ordinary Portland Cement concrete.
7. The cracks that were introduced deliberately before the exposure were still present and were found to have relatively large crack widths, extending deeply into the specimens. Some were found to have a reduced width at the specimen surface. It is concluded that no significant healing of these cracks had occurred during 16 years exposure to North Sea water, probably because of the absence of water flow through the cracks. Low-magnification fluorescence microscopy (FMA) of polished and resin-impregnated sections proved to be a useful technique to study the crack patterns inside the concrete.

## References

- ARUP, H., 1983, The mechanisms of the protection of steel by concrete, Proc. Corrosion of reinforcement in concrete construction, ed. A.P. Crane, SCI/Ellis Horwood, Chichester, 151–157.
- BAMFORTH, P.B., CHAPMAN-ANDREWS, J., 1994, Long term performance of RC elements under UK coastal conditions, Proc. Int. Conf. on Corrosion and Corrosion Protection of Steel in Concrete, ed. R.N. Swamy, Sheffield Academic Press, Sheffield, 139–156.

- BAMFORTH, P.B., 1994, "Specification and design of concrete for the protection of reinforcement in chloride contaminated environments", Proceedings Eurocorr/UKCorrosion94, Bournemouth, Institute of Materials/European Federation of Corrosion, 249–258.
- BIJEN, J.M.J.M., WEGEN, G.J.L. VAN DER, 1992, Behaviour of concrete affected by sea-water under high pressure, CUR, Gouda, The Netherlands, report 159, in Dutch with a summary in English.
- CLAYTON, N., 1986, Concrete strength loss from water pressurisation, Marine Concrete '86, London, The Concrete Society, 177–186.
- MILLARD, S. GHASSEMI, M. BUNGEY, J., JAFAR, M., 1990, Assessing the electrical resistivity of concrete structures, Proc. Corrosion of Reinforcement in Concrete, eds. C.L. Page, K.W.J. Treadaway, P.B. Bamforth, Elsevier, 303–313.
- POLDER, R.B., KETELAARS, M.B.G., 1991, Electrical resistance of blast furnace slag cement and ordinary portland cement concretes, Proc. Int. Conf. Blended Cements in Construction, ed. R.N. Swamy, Elsevier, 401- 415; TNO report BI-91–167, Rijswijk.
- POLDER, R.B., 1990, Prediction of corrosion protection by new concrete types in marine environment, SMOZ report 34/TNO report BI-90-086, in Dutch with a summary in English.
- POLDER, R.B., BAMFORTH, P.B., BASHEER, M., CHAPMAN-ANDREWS, J., CIGNA, R., JAFAR, M.I., MAZZONI, A., NOLAN, E., WOJTAS, H., 1994, Reinforcement Corrosion and Concrete Resistivity- state of the art, laboratory and field results -, Proc. Int. Conf. on Corrosion and Corrosion Protection of Steel in Concrete, ed. R.N. Swamy, Sheffield Academic Press, 571–580.
- POLDER, R.B., LARBI, J.A., 1995, Investigation of concrete exposed to North Sea water submersion for 16 years, TNO report 94-BT-R1548, to be published by CUR, Gouda, The Netherlands.
- RAIL, R.D., WENDT, R.L., 1985, Long-term, deep-ocean test of concrete spherical structures - results after 13 years, Naval Civil Engineering Laboratory Technical Report R-915.
- RAUPACH, M., 1992, Zur chloridinduzierten Makroelementkorrosion von Stahl in Beton, Deutscher Ausschuss für Stahlbeton, 433, Beuth Verlag, Berlin, in German with a summary in English.
- STILWELL, J.A., 1988, Exposure tests of reinforced concrete in sea water, Concrete in the Oceans Technical Report no. 23, Her Majesty's Stationary Office, London.
- TONDI, A., POLDER, R.B., CIGNA, R., 1993, Concrete resistivity and corrosion rate of reinforcement in atmospheric conditions after one year, TNO report 93-BT-R0170.
- WILKINS, N.J.M., LAWRENCE, P.F., 1983, The corrosion of steel reinforcements in concrete immersed in seawater, Conf. Corrosion of reinforcement in concrete construction, ed. A.P. Crane, SCI/Ellis Horwood, Chichester, 119–142.